ELSEVIER

Physica B 221 (1996) 134–140

PHYSICA B

Surface X-ray diffraction on the potassium-induced reconstruction of the Ag(0 0 1) surface

H.L. Meyerheim[a,*], S. Pflanz[a], R. Schuster[b], I.K. Robinson[b]

[a] *Institut für Kristallographie & Mineralogie der Universität München, Theresienstraße 41, 80333 München, Germany*
[b] *Department of Physics, University of Illinois, Urbana, IL 61801, USA*

Abstract

Surface X-ray diffraction experiments have been performed on the K-induced super structures on Ag(0 0 1). Both, the (2×1) and the (3×1) superstructure which are formed at K-coverages of about 0.15 and 0.30 ML, are found to consist of missing row type reconstructions, where one and two Ag-rows are missing along $[1\,\bar{1}\,0]$, respectively. In both cases the K-atoms reside within the large grooves of the missing row structures. For the (2×1) structure we find the K-atoms adsorbed on bridge sites relative to second-layer Ag-atoms, thereby coordinated by six Ag-atoms (four first-layer Ag-atoms and two second-layer Ag-atoms) at a distance of 3.44 (5) Å. The consideration of anharmonic displacement factors for the top layer Ag atoms is necessary for the proper description of the structure, leading to a significant better agreement with the data as compared to pure harmonic refinement as expressed by the goodness of fit parameter (GOF = 0.93 versus GOF = 1.67). Allowing for anharmonic displacement parameters we determine a Ag interlayer spacing d_{12} which is contracted relative to the bulk spacing by only 3.2% instead of 12.7% if anharmonic contributions are neglected. In the (3×1) superstructure the K-atoms form staggered double rows along $[1\,\bar{1}\,0]$, in this way forming a distorted quasihexagonal overlayer. The K-atoms are located close to bridge sites to second layer Ag-atoms at a minimum distance of 3.55 (5) Å. Additional defects are found in the first Ag-layer. For this more open reconstruction the Ag-interlayer spacing, d_{12}, is contracted by about 10% confirming recent investigations on FCC (1 1 0) surfaces regarding the polarization-induced compression of the interlayer distances.

1. Introduction

Alkali metals (AMs) like K and Cs are known for a long time to induce reconstructions on a number of low index metal surfaces. Much interest has been focused on the (1 1 0) surfaces of FCC-metal surfaces such as Ni, Cu, Ag and Pd [1–4]. For these reconstructions a missing row (MR) geometry has been proposed and theoretical studies of the AM-adsorption on FCC (1 1 0) surfaces have suggested that the more open MR structure is related to a higher chemisorption energy for the large K-atoms, because the K-atoms can get a higher coordination number in this case [5]. Recently, surface X-ray diffraction experiments have been performed on the different Cs induced reconstructions of the Ag(1 1 0) and the Cu(1 1 0) surfaces [6, 7]. In the latter case a systematic trend of the reconstruction-induced compression of the first interlayer spacing d_{12} could be demonstrated indicating a decreasing interlayer spacing with increasing extent (i.e. openness) of the reconstruction. This was explained by an increasing electrostatic polarization in the surface, whereas simple coordination arguments fail to explain the results since in all structures the top-layer Cu-coordination is identical.

Several AM-induced reconstructions have also been reported for the FCC (0 0 1) surfaces of Ag and Cu

* Corresponding author.

0921-4526/96/$15.00
SSDI 0921-4526(95)00915-9

[8–10]. For K-adsorption on Ag(0 0 1) at room temperature, Okada et al. [8, 9] report a (2 × 1) reconstruction between 0.1 and 0.2 ML coverage and a (3 × 1) reconstruction above about 0.25 ML. The absolute coverage Θ is defined as the ratio of the number density of the K atoms relative to the (unreconstructed) Ag(0 0 1) surface atoms (1 ML = 1.2×10^{15} atoms/cm^2). Although MR geometries have been suggested for the (2 × 1) and the (3 × 1) reconstructions and are also assumed in theoretical calculations [11], the detailed surface structure is not known so far.

The X-ray surface structure analysis gives direct evidence for MR-type geometries of the (2 × 1) and (3 × 1) reconstructions on the Ag(0 0 1) surface, where K adsorption sites are determined within the grooves of the MR-structure confirming the principle of coordination site maximisation. However, a complete description of the surface structure requires the proper consideration of the structural disorder expressed by atomic displacement parameters (ADPs) [12] for the first-layer Ag-atoms and the adsorbed K-atoms. On the basis of the (2 × 1) reconstruction, the present analysis demonstrates the importance of anharmonic ADPs and their possible implications for the structural parameters. As in the case of the Cu(1 1 0) surface the interlayer distance decreases with the formation of a more open reconstruction.

2. Experiment

The Ag(0 0 1) surface was prepared by repeated cycles of Ar^+-ion sputtering (500 eV) and annealing at about 800 K. The K atoms were evaporated by thorougly outgassed SAES dispensers. Within the sensitivity of the Auger-electron spectrometer (AES) system, no traces of contaminants could be detected after evaporation. The X-ray scattering experiments were performed at the beamline X16A of the National Synchrotron Light Source (NSLS) in Brookhaven (New York, USA) using the UHV diffractometer described by Fuoss et al. [13]. In situ monitoring of half or third-order superlattice reflections during evaporation allowed the homogeneous preparation of the (2 × 1) and (3 × 1) reconstruction over the sample surface thereby avoiding the simultaneous presence of several reconstructions within the coverage regime between about $\Theta = 0.18$ and 0.25 ML [8]. After the preparation of the reconstructions at 330 K, the sample was cooled immediately. The X-ray diffraction experiments reported here were performed at about 210 K for the (2 × 1) surface and at about 190 K for the (3 × 1) surface. In both cases about 110 reflections were measured reducing to 39 and 37 symmetry-independent reflections for the (2 × 1) and (3 × 1) reconstruction, respectively. This includes four superlattice rods measured up to 3.0 Å^{-1} corresponding to a maximum out-of-plane momentum transfer of 1.95 reciprocal lattice units. Systematic errors were estimated by the reproducibility of symmetry equivalent reflections which were in agreement in the regime below 10% in most cases. The stability of the surface structure was controlled by frequent monitoring of several reflections during the data collection.

3. Results and discussion

Fig. 1 shows the z-projected Patterson function $P(u, v)$ calculated for the (2 × 1) and the (3 × 1) reconstruction on the basis of the in-plane data only. Due to the high symmetry (pmm2) of the surface structures, their basic features are directly evident by the inspection of $P(u, v)$. Positive maxima (solid lines) can be related to Ag and K atoms, intense negative maxima (dashed lines) correspond to Ag-defects as labeled in Fig. 1. Negative maxima appear since only fractional order reflections are included in the data analysis providing a picture of the difference structure relative to the average (1 × 1) structure [14].

Both, the (2 × 1) and the (3 × 1) reconstructions are characterized by MR geometries, where one and two Ag-rows are missing along [1 $\bar{1}$ 0], respectively. Due to the low scattering power of K and the low K-coverage

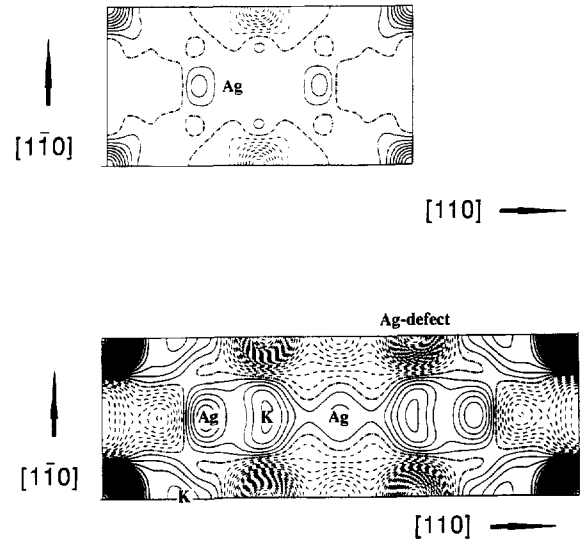

Fig. 1. Projected Patterson functions calculated for the (2 × 1) and the (3 × 1) reconstruction on the basis of the in-plane data. Positive maxima (solid lines) are related to Ag and K atoms as labeled. The intense negative maxima correspond to first layer Ag defects.

needed to form the (2 × 1) reconstruction, only the slightly shifted second-layer Ag atom is directly observable in the Patterson function. Direct inspection of the K adsorption site is obtained after least-squares refinement of the structure parameters by neglecting the K contribution and subsequent calculation of the difference Fourier synthesis [15] showing K to be located in the troughs of the MR-structure. In contrast, the K adsorption sites for the (3 × 1) reconstruction are directly observable in $P(u, v)$ which are close to bridge sites relative to the second layer Ag atoms. The least-squares refinement of the data sets was performed with the program "Prometheus" especially designed for the refinement of anharmonic thermal parameters [16]. Recently, the importance of anharmonic contributions to the thermal vibrations could be shown for Cs adorbed on Cu(0 0 1) forming a quasihexagonal monolayer [17]. In the present investigation we concentrate the discussion mostly on the (2 × 1) reconstruction; a more detailed investigation of the (3 × 1) reconstruction will be shown elsewhere [15].

Fig. 2 schematically shows in top and side view the structure of the (2 × 1) reconstruction. Top and second-layer Ag atoms labeled by $Ag_{(1)}$ and $Ag_{(2)}$ are indicated by small hatched and open circles, respectively, large circles represent K-atoms. One (2 × 1) unit cell is indicated by the rectangle shown in the upper right part of the topview drawing. Since the K coverage is only about 0.15 ML (i.e. 0.30 K-atoms per (2 × 1) unit cell), K atoms are shown to statistically occupy 30% of the (2 × 1) unit cells thereby leaving 70% of the surface unit cells empty. The K atoms are located at the centers of the (2 × 1) unit cells, however, a large anisotropic disorder is observed which can be taken into account by anisotropic thermal vibrations (dynamic model) or by partially occupied split positions (static model). In Fig. 2 the dynamic model is shown indicating the in-plane disorder schematically by an ellipse representing the K-disorder by anisotropic (harmonic) mean-square displacements U^{11}, U^{22} and U^{33} parallel to [1 1 0], [1 $\bar{1}$ 0] and [0 0 1], respectively [18]. Without temperature-dependent measurements it is not possible to distinguish between static and dynamic disorder, therefore in the present analysis the term 'atomic displacement parameters' (ADPs) will be used. Temperature-dependent data will be published elsewhere [15].

Table 1 summarizes the results of the structure refinement. In the first attempt we allowed only for harmonic ADPs to take account of the K and the top-layer $Ag_{(1)}$ disorder as indicated by the column "harmonic refinement". Very large ADPs are especially observed for the top-layer Ag-atoms normal to the sample surface and for K along the troughs of the MR structure parallel to [1 $\bar{1}$ 0]. The in-plane $Ag_{(1)}$ vibrations are larger by a factor of three parallel to [1 1 0] than along [1 $\bar{1}$ 0] which can be easily correlated with the anisotropic coordination of the Ag atoms within the top layer. The K–Ag bond lengths are in the regime between 3.40 and 3.50 Å, corresponding to an effective K-radius of about 2.0 Å if a metallic Ag radius of 1.44 Å is assumed. An interlayer spacing d_{12} of 1.78 ± 0.10 Å is derived for the (2 × 1) reconstruction corresponding to a contraction of 12.7% as compared to the bulk interlayer spacing (2.043 Å).

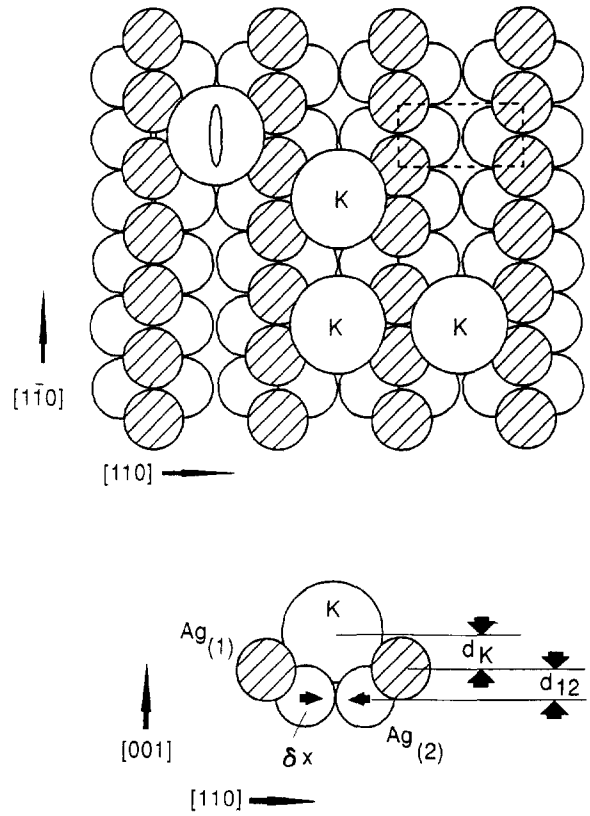

Fig. 2. Schematic drawing of the K/Ag(0 0 1) (2 × 1) reconstruction in top and side view. Top and second layer Ag-atoms ($Ag_{(1)}$, $Ag_{(2)}$) are shown by small hatched and open circles, respectively. Large circles represent K atoms. The ellipse in the upper left indicates the anisotropy of the in-plane root mean square displacement of the K atoms within the rows. The (2 × 1) unit cell is indicated by the dashed rectangle (a_0 = 5.78 Å, b_0 = 2.89 Å).

Although the structure parameters appear quite reasonable at first inspection, the goodness of fit parameter GOF is only 1.67 [19] indicating that there is still room for improvements. Since the consideration of a third Ag layer did not lead to an improvement of the fit and to reasonable results we tried a structure refinement including anharmonic ADPs. This looks especially justfied in view of

Table 1
Structure parameters derived for the K/Ag(0 0 1) (2 × 1) reconstruction allowing for harmonic (left column) and anharmonic (right column) atomic displacement factors of the top-layer Ag atoms

Structure	Harmonic	Anharmonic
K-occupancy factor	0.249 ± 0.067	0.397 ± 0.062
d_K (Å)	1.34 ± 0.16	1.17 ± 0.05 (Mean)
K–Ag_1 (Å)	3.50 ± 0.15	3.43 ± 0.05 (Mean)
K–Ag_2 (Å)	3.43 ± 0.19	3.44 ± 0.05 (Mean)
δ_x ($\times 10^2$ Å)	3.20 ± 0.30	3.60 ± 0.30 (Mean)
$Ag_{(1)}$–$Ag_{(2)}$ (Å)	2.72 ± 0.10	2.86 ± 0.05 (Mean)
d_{12} (Å)	1.78 ± 0.10	1.98 ± 0.05 (Mean)
d_{12} (Å)	1.78 ± 0.10	1.96 ± 0.05 (Mode)
Atomic displacement parameters		
$Ag_{(1)}$:		
U^{11} (Å^2)	0.048 ± 0.009	0.048 ± 0.009
U^{22} (Å^2)	0.007 ± 0.002	0.014 ± 0.002
U^{33} (Å^2)	0.117 ± 0.021	0.508 ± 0.045
C^{113} ($\times 10^3$)	—	0.783 ± 0.269
C^{333} ($\times 10^3$)	—	− 20.950 ± 3.560
D^{1111} ($\times 10^4$)	—	0.073 ± 0.034
D^{1122} ($\times 10^4$)	—	0.032 ± 0.018
D^{1133} ($\times 10^4$)	—	1.362 ± 0.387
$Ag_{(2)}$		
B (Å^2)	0.63 ± 0.36	1.84 ± 0.32
K		
U^{11} (Å^2)	0.020[a]	0.021 ± 0.019
U^{22} (Å^2)	0.216 ± 0.200	0.392 ± 0.211
U^{33} (Å^2)	0.020[a]	0.020[a]
Agreement parameters		
R_w	0.058	0.029
R_u	0.091	0.047
GOF (χ^2)	1.670	0.938

Note: The atoms are labeled according to Fig. 2. The terms "mean" and "mode" refer to the different definitions of the atomic position for $Ag_{(1)}$ in the case of anharmonic refinement.
[a] Parameters kept fixed during the refinement.

the large out-of-plane harmonic ADP ($U^{33} = 0.117$ Å^2) determined for $Ag_{(1)}$ which corresponds to a root mean square vibration of about 0.34 Å if it is interpreted in the dynamic model. Anharmonic effects were not found to be significant for K and the second layer Ag-atom. Anharmonic ADPs are taken into account by the Gram–Charlier (GC) series expansion of the harmonic (Gaussian) probability density function, $PDF_H(\boldsymbol{u})$ [12, 20, 21]:

$$PDF_{GC}(\boldsymbol{u}) = PDF_H(\boldsymbol{u}) \cdot \left[1 + \frac{1}{3!} C^{klm} H_{klm}(\boldsymbol{u}) + \frac{1}{4!} C^{klmn} H_{klmn}(\boldsymbol{u}) + \cdots \right], \quad (1)$$

where $\boldsymbol{u}$ represents the displacement vector from the minimum potential position $\boldsymbol{u}_0$ (mode position, see below). The multidimensional Hermite polynomials $H_{klmn\ldots r}(\boldsymbol{u})$ are the r^{th}-order derivatives of $PDF_H(\boldsymbol{u})$ with respect to $\boldsymbol{u}$. The Fourier transform of Eq. (1) leads to a generalized ADP (temperature factor) $T_{GC}(\boldsymbol{h})$ which is given by a series expansion of the harmonic ADP, $T_H(\boldsymbol{h})$:

$$T_{GC}(\boldsymbol{h}) = T_H(\boldsymbol{h}) \left[1 + \frac{(2\pi \mathrm{i})^3}{3!} h_k h_l h_m C^{klm} + \frac{(2\pi)^4}{4!} h_k h_l h_m h_n D^{klmn} + \cdots \right]. \quad (2)$$

Using this equation a generalized expression for the structure factor is obtained:

$$F_{GC}(\boldsymbol{h}) = \sum_j f_j \, e^{i 2\pi h_k x_j^k - 8\pi^2 U_j^{kl} h^k h^l} \left[1 - i \tfrac{4}{3} \pi^3 h_k h_l h_m C_j^{klm} + \tfrac{2}{3} \pi^4 h_k h_l h_m h_n D_j^{klmn} - \cdots \right], \quad (3)$$

where the h_j correspond to the reflection indices ($j = 1, 2, 3$) and the sum convention has to be applied. The anharmonic corrections for the atom j in the structure factor equation are given up to the fourth order by the higher-order (dimensionless) tensor coefficients C_j^{klm} and D_j^{klmn}. The first- and second-order terms of the series expansion are set to zero, meaning that the average and the standard deviation of the harmonic part include the anharmonic first- and second-order contributions.

It is worth mentioning that whenever anharmonic terms are involved in the calculation of the temperature factor, respectively, the corresponding PDFs and the effective one particle potentials (OPPs) [12, 16, 20], a distinction has to be made between different expressions for the atomic positions. The mean position is just simply the refined first-order term in the series expansion. The so-called "mode position" is given by the minimum of the OPP, the latter is given by $V(\boldsymbol{u}) = -kT \ln[PDF(\boldsymbol{u})/PDF(\boldsymbol{u}_0)]$. Therfore, the mode position corresponds to $\boldsymbol{u} = \boldsymbol{u}_0$, the maximum of the PDF. The physical mostly important positional parameter is the equilibrium position, $M(\boldsymbol{u})$ which is the true mean position of an atom at a given temperature. $M(\boldsymbol{u})$ can be evaluated using the calculated OPP by $\int \boldsymbol{u} e^{-V(u)/kT} du / \int e^{-V(u)/kT} d\boldsymbol{u}$, corresponding to the quantum mechanical expectation value of $\boldsymbol{u}$. Only in the harmonic case the mean, mode and equilibrium positions are identical. If only even-order terms of the general structure factor, Eq. (3), are involved, at least the mean and the equilibrium position are identical. In the presence of odd-order modifications (as discussed here) the mean, mode and equilibrium positions may differ. In the present investigation we confine ourselves to the discussion of the mean and mode position, since the

evaluation of the equilibrium position requires the analysis of the detailed shape of $V(\boldsymbol{u})$, whose physical significance can only be checked by temperature-dependent data which will be discussed in a separate paper [15].

Symmetry restrictions considerably reduce the number of anharmonic refinement parameters. Out of a maximum of 10 third-order and 15 fourth-order coefficients in the general case, only 3 third-order (C^{333}, C^{113} and C^{223}) and 6 fourth-order coefficients (D^{1111}, D^{2222}, D^{3333}, D^{1122}, D^{1133}, D^{2233}) remain as fitting parameters for $Ag_{(1)}$. Further, 4 coefficients were rejected as insignificant (and set to zero) as their standard deviations are of the order of 60–100%. Table 1 summarizes the results on the right column. The refinement including anharmonic ADPs improves the fit by a factor of two independent of what agreement parameter is used [19]. Fig. 3 compares the structure factor amplitudes ($|F_{calc}|$) calculated for the anharmonic refinement with the observed ($|F_{obs}|$), showing overall good agreement of the fit with the data.

The standard deviations of the anharmonic ADPs are generally below 50%, for C^{333} it is only 17%, therefore the refinement results can be considered as highly significant. In addition, the error bars for the structural parameters decrease with inclusion of anharmonic ADPs as compared to the harmonic refinement. However, the most interesting result is that in the anharmonic refinement the Ag interlayer spacing is contracted by only 3.2% ($d_{12} = 1.98 \pm 0.05$ Å) relative to the bulk interlayer spacing if we refer to the mean position of $Ag_{(1)}$ (see above). Nearly the same result is obtained if the distances are referred to the $Ag_{(1)}$ mode position ($d_{12} = 1.96 \pm 0.05$ Å), i.e. the maximum of the anharmonic PDF of $Ag_{(1)}$ is slightly below the mean atomic position. In the case of the anharmonic refinement, the interlayer spacing is therefore smaller than in the harmonic case where the contraction is 12.7%. Due to the pronounced deviation from a parabolic potential at large distances from the surface a similar result can qualitatively also be suspected if the equilibrium position $M(\boldsymbol{u})$ of $Ag_{(1)}$ is considered (see Fig. 4 and Ref. [15]). In the context of the distance determination it is important to note that the positional Ag parameters and the ADPs of $Ag_{(1)}$ are *not* strongly coupled in the fit, the maximum correlation being 0.46. Therefore, it can be concluded that neglecting the anharmonic part of the ADPs of the highly disordered top-layer Ag-atom leads to an artificial large compression of the first interlayer spacing. In contrast, the K–Ag distances are not strongly affected in the present case.

A direct representation of the ADPs is possible by calculating the PDFs for both, the harmonic and the anharmonic refinements. This is shown in Fig. 4 where the PDFs of the first- and second-layer Ag-atoms are shown in a plane that is spanned by vectors parallel to [1 0 0] and [0 0 1]. The section of the plane with the (0 0 1)

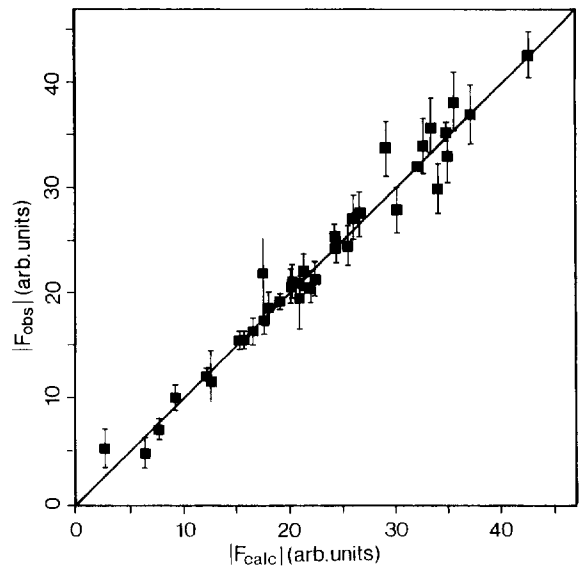

Fig. 3. Plot of $|F_{obs}|$ versus $|F_{calc}|$ for the anharmonic refinement ($R_w = 2.9\%$, GOF = 0.94).

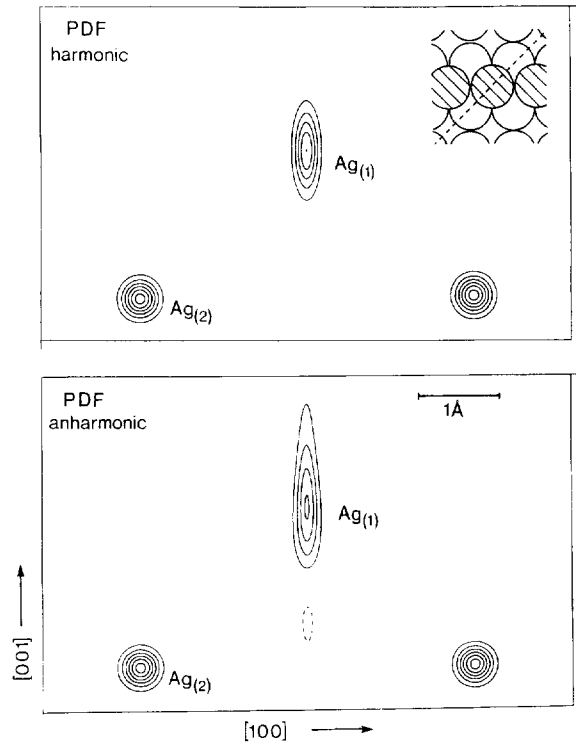

Fig. 4. Probability density function $Ag_{(1)}$ and $Ag_{(2)}$ for the harmonic and anharmonic refinement in a plane defined by vectors parallel [1 0 0] and [0 0 1]. The section of the plane with the (0 0 1) surface is given by the dashed line in the inset.

surface is indicated by the dashed line in the inset of Fig. 4. For $Ag_{(1)}$ a significant deviation of the PDF from the (harmonic) ellipsoidal shape is observed along [0 0 1] which can be attributed to the large magnitude of the C^{333} coefficient. In the context of a dynamic disorder model, the elongation of the PDF parallel [0 0 1] can be interpreted by a large anharmonic vibration indicating a weak bonding of the $Ag_{(1)}$ atoms to the four second-layer Ag-atoms. In view of the results of the (3×1) structure analysis we may speculate that this pronounced disorder might be related to a "precursor" state close to the $(2 \times 1) \rightarrow (3 \times 1)$ phase transition which involves a thorough rearrangement of the surface Ag-atoms. A more detailed discussion of the PDFs and the corresponding effective one-particle potentials needs the analysis of temperature-dependent data [15].

Finally, we shortly discuss the (3×1) reconstruction which is shown in Fig. 5. Good agreement with the data ($R_w = 0.038$, GOF = 1.14) is obtained by assuming K to be adsorbed statistically at two different sites labeled by $K_{(1)}$ and $K_{(2)}$ both of which are close to bridge sites relative to second layer Ag-atoms. In principle, the structure can be described as a densely packed distorted quasihexagonal overlayer. As in the case of the (2×1) reconstruction the $K_{(1)}$ atoms are strongly disordered along $[1\bar{1}0]$ which can be static or dynamic in nature. We find $U^{22} = 0.84$ Å^2, a value which is too large to be due to simple harmonic disorder. However, anharmonic refinement was not significant in this case; therefore it is a reasonable assumption to take account of split atoms

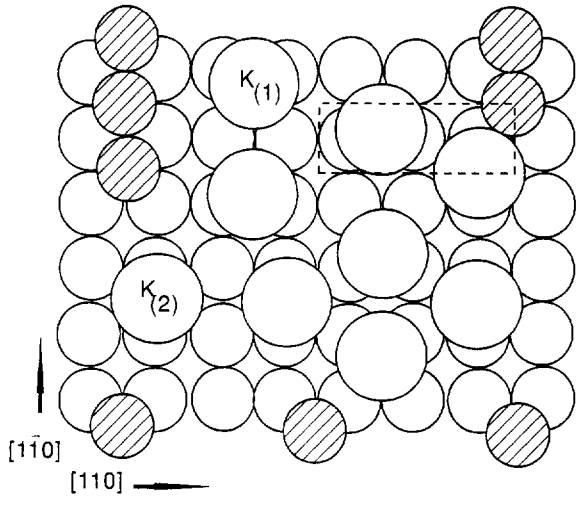

Fig. 5. Schematic drawing of the K/Ag(0 0 1) (3×1) reconstruction. The Ag atoms are indicated as in Fig. 2. The K atoms adsorbed statistically at two different sites are labeled by $K_{(1)}$ and $K_{(2)}$, respectively.

(static disorder), i.e. two different adsorption sites slightly off the bridge sites as shown in Fig. 5. In this case we find $K_{(1)}$ at $x = 0.33$, $y = 0.34$ within the (3×1) unit cell shown as dashed rectangle in the upper right part of the figure ($K_{(2)}$ at $x = 0.17$, $y = 0.00$). For both K-atoms nearest bond lengths to Ag are in the range 3.5–3.6 Å. In addition to two missing Ag-rows a number of additional Ag-defects (about 60%) in the first layer have to be assumed if the K-coverage is kept fixed at about 0.30 ML. Anharmonic ADPs for the top-layer Ag-atoms are also important; however, only two third-order coefficients were found to be significant. Most importantly, in comparison to the (2×1) reconstruction the Ag interlayer spacing d_{12} is considerably more contracted by about 10% relative to the bulk spacing. This result is in good correspondence with recent systematic invesitgations relating the degree of the interlayer compression to the openness of the reconstruction [7].

4. Summary

In summary, we have presented an X-ray structure analysis of the K-induced reconstruction of Ag(0 0 1). Both, the (2×1) and the (3×1) reconstructions are characterized by missing row geometries with one or two rows of Ag atoms along $[1\bar{1}0]$ missing, respectively. Definite K adsorption sites close to bridge sites with respect to second-layer Ag-atoms were determined in all cases. From the derived bond lengths which generally are in the regime between 3.4 and 3.6 Å an effective K radius of about 2.0 Å is derived. The consideration of anharmonic displacement parameters is found to be of crucial importance for the proper description of the structure. For the (2×1) reconstruction we have given evidence for the first Ag interlayer spacing to be determined to be too compressed if only harmonic terms are included in the refinement. Nevertheless, we find a systematic compression of the interlayer spacing with increasing extent of the reconstruction. This confirms recent investigations on the Cs induced reconstruction of Cu(1 1 0).

Acknowledgements

We (S.P. and H.L.M.) would like to thank AT&T for providing access to the beamline X16A and their hospitality during their visit in Brookhaven. The support of the Bundesministerium für Wissenschaft und Forschung under Grant #05464IAB8 is gratefully acknowledged. Work at the NSLS was supported by the US Department of Energy under DE-AC 012-76CH0016. Additional support came from the University of Illinois Mat. Res. Laboratory under grant DEFG02-91ER45439.

References

[1] B.E. Hayden, K.C. Prince, P.J. Davies, G. Paolucci and A.M. Bradshaw, Solid State Commun. 48 (1983) 325.

[2] C.J. Barnes, M.Q. Ding, M. Lindroos, R.D. Diehl and D. King, Surf. Sci. 162 (1985) 59.

[3] S.M. Francis and N.V. Richardson, Surf. Sci. 152/153 (1985) 63.

[4] R.J. Behm, G. Ertl, D.K. Flynn, K.D. Jamison and D.A. Thiel, Phys. Rev. B 36 (1987) 9267.

[5] K.W. Jacobson and J.K. Nørskov, Phys. Rev. Lett. 60 (1988) 2496.

[6] R. Schuster, P.J. Eng and I.K. Robinson, Surf. Sci. 326 (1995) L477.

[7] R. Schuster and I.K. Robinson, in press.

[8] M. Okada, H. Tochihara and Y. Murata, Phys. Rev. B 43 (1991) 1411.

[9] M. Okada, H. Tochihara and Y. Murata, Surf. Sci. 245 (1991) 380.

[10] S. Mizuno, H. Tochihara and T. Kawamura, Surf. Sci. 292 (1993) L811.

[11] O.B. Christensen and K.W. Jacobson, Phys. Rev. B 45 (1992) 6893.

[12] W.F. Kuhs, Acta Cryst. A 48 (1992) 80.

[13] P.H. Fuoss and I.K. Robinson, Nucl. Instr. Meth. 222 (1984) 171.

[14] M.J. Buerger, Vector Space (Wiley, New York, 1959).

[15] H.L. Meyerheim, S. Pflanz, R. Schuster and I.K. Robinson, to be published.

[16] U.H. Zucker, E. Perenthaler, W.F. Kuhs, R. Bachmann and H. Schulz, J. Appl. Cryst. 16 (1983) 358.

[17] H.L. Meyerheim, W. Moritz, H. Schulz, P.J. Eng and I.K. Robinson, Surf. Sci. 331–333 (1995) 1422.

[18] We use a sample setting corresponding to a primitive (1×1) surface unit cell, therefore the a-, b- and c-axis of the surface unit cell is parallel to $[1\,1\,0]$, $[1\,\bar{1}\,0]$ and $[0\,0\,1]$ of the FCC unit cell.

[19] I.K. Robinson, in: Handbook of Synchrotron Radiation, Vol. 3, eds. G.S. Brown and D.E. Moncton (Elsevier, Amsterdam, 1991).

[20] U.H. Zucker and H. Schulz, Acta Cryst. A 38 (1982) 563.

[21] C.K. Johnson and H.A. Levy, in: The International Tables for X-Ray Crystallography, Vol. IV (Kynoch Press, Birmingham, 1974).